UCRL-17146

University of California
Ernest O. Lawrence Radiation Laboratory

THE ANNEALING OF STACKING FAULT TETRAHEDRA IN GOLD

TWO-WEEK LOAN COPY

This is a Library Circulating Copy which may be borrowed for two weeks. For a personal retention copy, call Tech. Info. Division, Ext. 5545

Berkeley, California

DISCLAIMER

This document was prepared as an account of work sponsored by the United States Government. While this document is believed to contain correct information, neither the United States Government nor any agency thereof, nor the Regents of the University of California, nor any of their employees, makes any warranty, express or implied, or assumes any legal responsibility for the accuracy, completeness, or usefulness of any information, apparatus, product, or process disclosed, or represents that its use would not infringe privately owned rights. Reference herein to any specific commercial product, process, or service by its trade name, trademark, manufacturer, or otherwise, does not necessarily constitute or imply its endorsement, recommendation, or favoring by the United States Government or any agency thereof, or the Regents of the University of California. The views and opinions of authors expressed herein do not necessarily state or reflect those of the United States Government or any agency thereof or the Regents of the University of California.

Submitted to Philosophical Magazine

UCRL-17146
Preprint

UNIVERSITY OF CALIFORNIA

Lawrence Radiation Laboratory
Berkeley, California

AEC Contract W-7405-eng-48

THE ANNEALING OF STACKING FAULT TETRAHEDRA IN GOLD

M. J. Yokota and J. Washburn

September 1966

THE ANNEALING OF STACKING FAULT TETRAHEDRA IN GOLD

M. J. Yokota and J. Washburn

Inorganic Materials Research Division, Lawrence Radiation Laboratory
and Department of Mineral Technology, College of Engineering
University of California, Berkeley, California

ABSTRACT

The disappearance of stacking fault tetrahedra in 99.999% gold in the temperature range 175°C to 400°C was studied by transmission electron microscopy. In this temperature range, no shrinkage of tetrahedra was detected. Disappearance always took place by collapse to a triangular stacking fault loop and subsequent shrinkage of the loop. Because of a size dependence on the rate of disappearance, it is suggested that collapse of the tetrahedra usually occur by nucleation of a Shockley partial loop on a face or edge of the tetrahedron rather than at a corner. During shrinkage, the sides of the stacking fault loops remained straight and parallel to <110> which suggests that the 1/3<111> dislocation is dissociated. Many loops developed new <110> sides during shrinkage becoming 4, 5 or 6 sided. Even those loops that appeared to remain triangular probably developed short new sides at the corners because the reverse reaction (stacking fault triangle → tetrahedron) was never observed, even when the 1/3<111> loops had shrunk below the critical size at which the energy of a tetrahedron is less than that of the corresponding triangular stacking fault loop.

I. INTRODUCTION

Stacking fault tetrahedra can be formed by the clustering of vacancies or the cross-slipping of super-jogged dislocations. For the vacancy clustering process, two different mechanisms can be visualized: Tetrahedra may form directly by growth of tetravacancies as proposed by DeJong and Koehler (1963) or triangular Frank sessile loops may form first and later transform to stacking fault tetrahedra as suggested by Silcox and Hirsch (1959).

In the cross-slipping process, two mechanisms are also possible: A super-jogged dislocation can cross-slip to form a triangular Frank sessile loop which then could transform to a tetrahedron (Hirsch, 1962). Alternatively, a super-jogged dislocation might cross slip to form first a triangular perfect prismatic loop which then dissociates to form the stacking fault tetrahedron.

The disappearance of stacking fault tetrahedra during annealing may also occur by alternative mechanisms that correspond approximately to the reverse of the formation mechanisms. Thus, stacking fault tetrahedra can be thought to shrink and disappear by:

1) direct emission of vacancies at ledges in the stacking fault tetrahedra
2) collapse of the tetrahedra to Frank sessile dislocation loops with subsequent emission of vacancies from the loop.

or 3) collapse of tetrahedra to perfect prismatic loops followed by shrinkage of the perfect loop.

In the present experiments the annealing of tetrahedra of 50 to 2000Å in size was studied by following their disappearance in thin gold

foils by transmission electron microscopy. In order to achieve more accurate control of temperature, annealing of the thin foils was performed outside the microscope where the temperature could be controlled to ±2°C. The main purpose of the experiments was to determine which of the possible mechanisms of shrinkage is operative.

II. EXPERIMENTAL PROCEDURE

A. Specimen Preparation

Polycrystalline gold specimens suitable for quenching were prepared from 75 micron thick sheet material obtained from Cominco Products Inc. of Spokane, Washington. The manufacturer produced this sheet material from one-half inch thick slabs of chemical reduction refined 99.999% purity gold by cold rolling at room temperature approximately twenty times without any intermediate annealing. The impurity content as given by the manufacturer is listed in Table I. Specimens 25 mm long and 12 mm wide were prepared from this material and annealed in alumina boats at 1000°C for 48 hours in air and then allowed to cool slowly within the furnace. The resulting specimens had a <001> preferred orientation which is convenient because it allows easy differentiation between triangular Frank sessile loops and stacking fault tetrahedra. Triangular Frank sessile dislocation loops appear in this projection as triangles, while stacking fault tetrahedra appear as squares.

The specimens were next placed in quartz specimen holders and suspended in a vertical tube furnace open to the atmosphere. Specimens were quenched from a temperature of 1000°C. Quenching was performed by releasing the weighted specimen holder into an ice-water bath fixed

a few centimeters below the specimen. The specimens were then aged for 1, 2, 3 and 4 hours at one of the following temperatures: 0, 50, 100 or 150°C ± 2°C. The time spent in transferring the specimen from the quenching bath to the aging bath was kept constant at 30 seconds. Both silicon oil and water were used as heat transfer mediums for the aging bath. After completion of the aging treatment, the specimens were stored in absolute ethyl alcohol at 0°C. The different sizes and densities of tetrahedra that could be obtained by varying the aging temperature are shown in Fig. 1.

B. Thin Foil Preparation

Thin foil samples suitable for observation under the electron microscope were prepared by electropolishing utilizing a modification of the standard window technique. The specimens were mounted in noncorrosive holders so as to minimize plastic deformation of the specimens due to handling during the electrothinning step. A controlled rate of flow of the polishing solution past the two faces of the specimen was achieved by the use of a pair of parallel plate stainless steel cathodes of adjustable width and a magnetic stirrer. The temperature of the cell was controlled by a constant temperature bath.

A two step electrothinning procedure was used. The compositions of the two polishing solutions as well as the temperatures and current densities used are listed in Table II. The more reactive hydrochloric acid-solution was used to thin the specimens down to approximately a micron while the less reactive, more controllable chromic-oxide acetic

acid solution was used to produce the final thin foils. At no time during the entire thinning process was the specimen subjected to temperatures higher than room temperature. Near the final stages of the thinning process the current was switched on and off repeatedly. This caused small flakes to separate at the edges of the specimen which were then recovered from the solution, rinsed and stored in ethyl alcohol at 0°C.

C. Electron Microscope Technique

A Siemens 1 electron microscope, operated at 100 kv with a beam current less than 20μa, was used to make all of the microscope observations. Tilting experiments were facilitated by the use of a two axis tilting stage. For the annealing performed outside the microscope a detachable specimen cap constructed of gold was used. Gold grids were also used to further minimize contamination and avoid plastic deformation of the specimen by differential thermal expansion.

III. RESULTS AND DISCUSSION

A. Thin Foil Annealing Experiments

Figures 2a and b are micrographs taken of an area before and after 30 minutes annealing at a temperature of 175°C. Note that the complete stacking fault tetrahedra (1) and (3) which appear as squares in Fig. 2a, have become triangular Frank sessile dislocation loops in Fig. 2b. This same collapse has occurred for the stacking fault tetrahedron (2) that cuts one of the surfaces of the foil. The resulting Frank sessile dislocation loop in this case is a trapezoid.

The collapse of stacking fault tetrahedron (4) may have been aided by the stress field of a dislocation (5). For the other three examples, however, the resulting Frank loops do not lie on the same plane, suggesting that stresses that may have been present during annealing did not aid significantly in their collapse.

The tetrahedra in Fig. 2 were in the size range 1000 - 2000Å. Smaller tetrahedra, on the order of 100 - 200Å generally required higher temperatures and/or longer times for collapse. Figures 3a, b, c and d are micrographs taken of an area annealed for a) 0, b) 30, c) 60 and d) 90 minutes at 400°C showing the collapse of smaller stacking fault tetrahedra to triangular Frank sessile loops. Reactions can be seen at the positions which have been circled. Emission of vacancies occurs after collapse of the tetrahedron by the shrinkage of the resulting loop as shown in Fig. 4. Figure 5 shows a complete sequence of annealing steps at a temperature of 300°C. See positions (5) and (6) in Fig. 6. Here, stacking fault tetrahedra which appear as squares can be seen to collapse to triangular Frank sessile dislocation loops which then shrink and disappear upon continued annealing. Further examples of the shrinking of Frank sessile dislocation loops can be seen at positions 1, 2, 3 and 4. Note that some of these loops have retained their original triangular shape during shrinking while others have become four, five or six-sided.

For the loops that have remained triangular during annealing, it is interesting to note that the Silcox-Hirsch reaction: stacking fault

loop → stacking fault tetrahedron apparently does not take place even after the loop has certainly shrunk below the critical size ℓ_c where the stacking fault tetrahedron becomes stable relative to the Frank sessile dislocation loop. This is particularly surprising because the Frank sessile dislocation may be extended; the fact that loop edges remain straight and parallel to <110> during shrinkage suggests that they are (see Figs. 4 and 5). For an extended triangular Frank sessile dislocation loop, there should be little or no activation energy needed to complete the stacking fault tetrahedron once the loop has shrunk well below the critical size. However, if steps are formed in the loop, like the one in Fig. 4, or if the loop has become 4, 5, or 6 sided during annealing, reformation of the tetrahedron may be difficult even within the size range where the stacking fault tetrahedron has a lower energy than the corresponding Frank sessile dislocation loop.

B. Dislocation - Stacking Fault Tetrahedra Interaction Experiments

Figure 6a shows several dislocations that have moved up against a stacking fault tetrahedron (A). Figure 6b shows the same area moments later. Here, the stress field of the several dislocations has probably helped to cause the collapse of the stacking fault tetrahedron onto the face that is farthest from the stress field of the dislocation. The new configuration is a triangular Frank sessile dislocation loop.

The reaction that has taken place can be seen more clearly through the schematic illustration, Fig. 7a, b, c, and d. In Fig. 7a, an extended dislocation is being held up by the stacking fault tetrahedron BDAC. In Fig. 7b, the stress field of the dislocation helps to nucleate the

Schockley partials αB and $B\delta$ at the stair rod $\alpha\delta$ by decreasing the critical radius above which the Shockley loop becomes stable. Figure 7c shows an intermediate state of collapse. Figure 7d shows the final product, the triangular Frank sessile dislocation loop on the face CDA of the original stacking fault tetrahedron.

C. Rate of Annealing

If it is assumed that the disappearance of tetrahedra in gold involves the reaction:

1) SFT → FSL

the rate of disappearance of tetrahedra should be

$$R = k_1 \, [SFT]$$

where [SFT] is the concentration of stacking fault tetrahedra and k_1 has the form

$$k_1 = Ae^{-(\Delta E+E^*)/kT}$$

E^* = activation energy for the reaction

ΔE = difference in energy between the SFT and FSL for the same value of ℓ, the edge length, and temperature, T.

A = pre-exponential factor which includes a frequency factor, the number of sites at which a Shockley partial can nucleate and the entropy of activation

For SFT of edge length greater than ℓ_c, the expression for the rate constant reduces to

$$k_1 = Ae^{-E^*/kT}$$

To be able to predict the rate of annealing of SFT, it is necessary to make an estimate of the activation energy.

Three mechanisms for the reaction SFT → FSL can be visualized, each involving the nucleation of one or more Shockley partial dislocations. The first mechanism involves the nucleation of a Shockley partial dislocation loop in one of the four faces of the stacking fault tetrahedron. The total energy of the loop, E, can be expressed as the sum of three separate energy terms.

$$E_f = E_L(r \ln r) - E_{SF}(r^2) - W_\tau(r^2)$$

where

E_L = energy of the dislocation loop formed (proportional to r ln r).

E_{SF} = energy of the stacking fault destroyed in the formation of the loop (proportional to r^2).

W_τ = work done by the external stress field, τ, as the dislocation loop expands. This stress can also be provided by a dislocation.

E_f has a maximum value at the critical radius r_c which must be supplied by a thermal fluctuation to nucleate a stable Shockley loop. This mechanism was first proposed by Meshii and Kauffman (1960) in order to explain the results of their annealing experiments. They obtained an experimental value of 4.7 eV for the activation energy of the annealing process which agreed well with their calculated value of 6.6 eV based on the above model.

The second mechanism involves the nucleation or dissociation of two Shockley partial dislocations from one of the stair rod dislocations. The activation energy for this mechanism has a form similar to the preceding case.

$$E_e = E_L - E_{SF} - W_\tau - E_{SR}(r)$$

where E_L, E_{SF} and W_τ have the same meanings as in the previous case.

E_{SR} = energy of the length of stair rod dislocation destroyed in the formation of the two Shockley partial dislocations.

If nucleation takes place in this manner, the value of the activation energy, E^*, for collapse should be slightly smaller than for the preceding case, because of the length of stair rod dislocation that is destroyed. However, the number of sites where the process can occur is very much smaller. For face nucleation, the number of sites available for the nucleation of a Shockley partial dislocation loop is proportional to ℓ^2 where ℓ is the edge length of the tetrahedron. For edge or stair rod nucleation, the number of sites is proportional to ℓ.

The third possible mechanism involves the nucleation or dissociation of three Shockley partial dislocations from a corner of the tetrahedron where three stair rod dislocations meet. The expression for the activation energy, E_c, based on this model has the same form as case II discussed above. The activation energy for this mechanism is expected to be slightly lower than either of the preceding mechanisms but, the number of nucleation sites is only 4, the corners of the tetrahedron.

The measured activation energy in a macroscopic annealing experiment may well be influenced by all three mechanisms and must be related by the expression

$$k = A_c e^{-E_c^*/kT} + A_e e^{-E_e^*/kT} + A_f e^{-E_f^*/kT}$$

The dominance of any particular mechanism would be dependent on the pre-exponential term, A, as well as the activation energy E. Because

$$A_c << A_e << A_f$$

and

$$E_c < E_e < E_f$$

it is conceivable that each of the three mechanisms could dominate over a particular temperature range. For the temperature range 200 → 400°C and for the larger sized stacking fault tetrahedra > 1000Å studied in these experiments there appeared to be a strong size dependence on the annealing rate. See, for example, Fig. 2 where the stacking fault tetrahedra that have collapsed are all among the largest of those present. This also appears to be the case for the bulk annealing that occurs during the aging treatment. Most of the triangular Frank sessile dislocation loops in Figs. 1c and d probably resulted from collapse of stacking fault tetrahedra. This size dependence on the stacking fault tetrahedra collapse rate indicates the dominance of either the face or edge mechanism.

The collapse of tetrahedra to triangular Frank loops was not observed in the recent studies of Segall et al. (1966) and Shimomura et al. (1966). A possible explanation may be that at the higher annealing temperatures of their studies the lifetime of the Frank sessile loops formed by the collapse of small stacking fault tetrahedra ∿200Å would be very short.

IV. CONCLUSIONS

(1) On heating of 99.999% pure gold containing stacking fault tetrahedra into the temperature range 175° to 400°C, none of the tetrahedra were observed to shrink in size.

(2) Disappearance of tetrahedra takes place by collapse to

triangular stacking fault loops and subsequent emission of vacancies from the loop.

(3) The collapse takes place by nucleation of a Shockley partial loop either on one of the faces or along an edge of the tetrahedron.

(4) The edges of the stacking fault loops remain parallel to <110> during shrinkage but in many cases the loops become noticeably 4, 5 or 6 sided during shrinkage. This suggests that the 1/3<111> dislocations are dissociated.

(5) Even those loops that appear to remain triangular during shrinkage probably develop short new sides at the corners because the reverse reaction (triangular stacking fault loop → stacking fault tetrahedron) is never observed even when the loop has shrunk to a size below which the tetrahedron must have a lower energy.

ACKNOWLEDGEMENTS

The authors are pleased to acknowledge the financial support of the United States Atomic Energy Commission through the Inorganic Materials Research Division of the Lawrence Radiation Laboratory, University of California in Berkeley. We also wish to thank Drs. J. A. Ytterhus and W. A. Westdorp for their help with regard to the electrothinning procedure.

Table I

Impurities	ppm
Platinum	2.0
Lead	1.0
Silver	0.5
Copper	0.3
Silicon	0.2
Iron	0.1
Magnesium	0.1

Table II

Electrolytic Solution No. 1	
Hydrochloric acid - HCl (37.5%)	200 cc
Ethyl alcohol - $C_2H_5(OH)$ (200 p)	175 cc
Glycerin - $C_3H_5(OH)_3$ (95.0%)	125 cc
Temperature: -30°C	
Current Density: 0.7 amp/cm^2	
Electrolytic Solution No. 2	
Glacial Acetic Acid - CH_3COOH (99.8%)	465 cc
Chromium Trioxide CrO_3	87.5 gms
Water H_2O	25 cc
Temperature: 10°C	
Current Density 0.25 amps/cm^2	

REFERENCES

DeJong, M. and Koehler, J. S., (1963) Phys. Rev., 129, 49.

Hirsch, P. B., (1962) Phil. Mag., 7, 67.

Meshii, M. and Kauffman, J. W., (1960) Phil. Mag., 5, 939.

Segall, R. L., Clarebrough, L.M. and Loretto, M. H. (1966) Phil. Mag., 14, 53.

Shimomura, Y., Kiritani, M., Yoshinaka, A. and Yoshida, S. (1966) Sixth International Congress for Electron Microscopy, Kyoto, p. 349.

Silcox, J. and Hirsch, P. B. (1959) Phil. Mag., 4, 72.

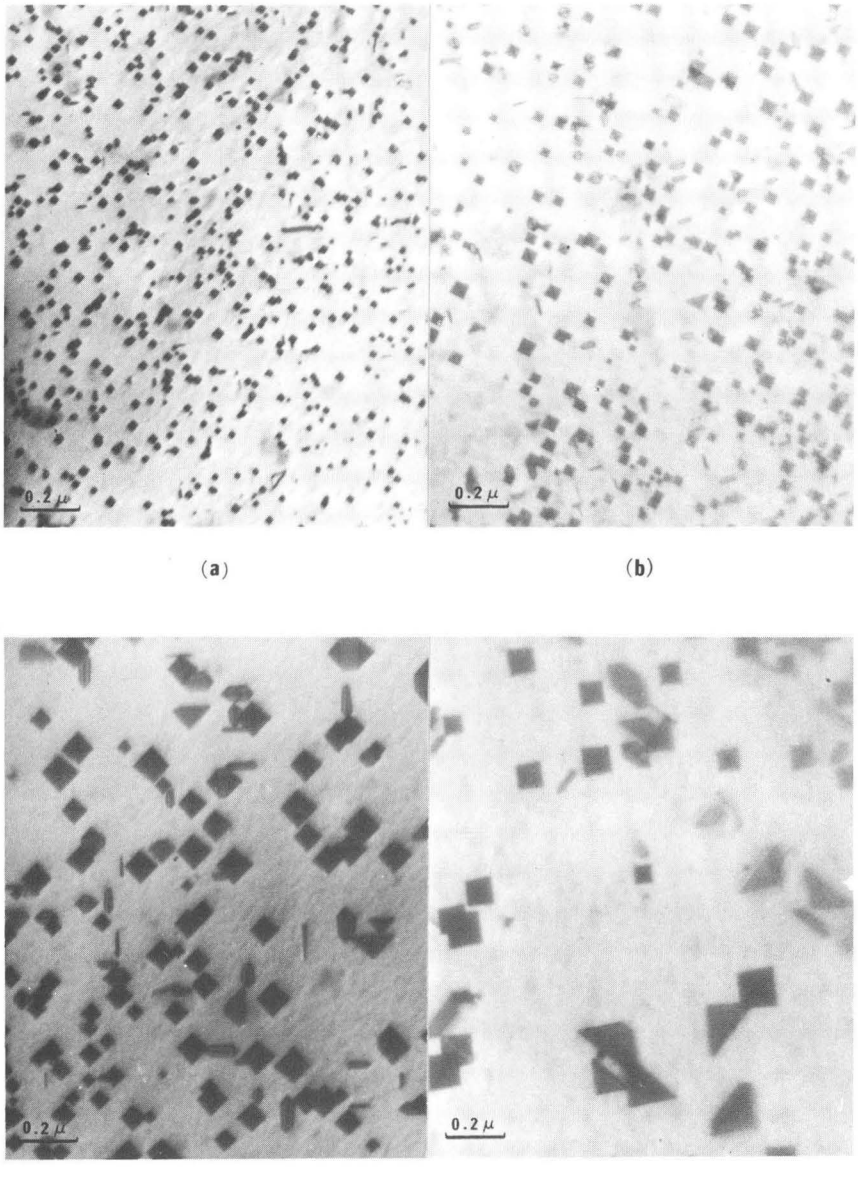

ZN-6031

Fig 1. Micrographs showing the stacking fault tetrahedra densities and size distributions obtained by varying the aging temperature a) 0°C, b) 50°C, c) 100°C and d) 150°C. Scale 0.2μ, mark = 1 cm.

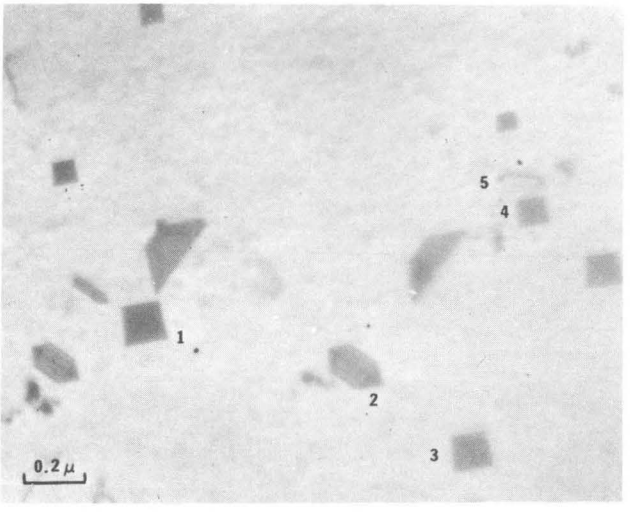

(a)

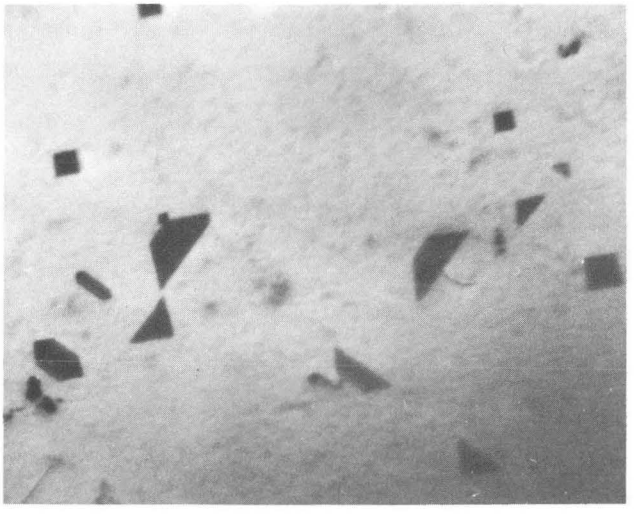

(b)

ZN-6036

Fig. 2. Micrographs taken of an area before and after 30 minutes annealing at 175°C showing the collapse of stacking fault tetrahedra to triangular Frank sessile dislocation loops. Note that collapse here seems to be size dependent in that only the very largest SFT have collapsed. Scale 0.2μ = 1 cm.

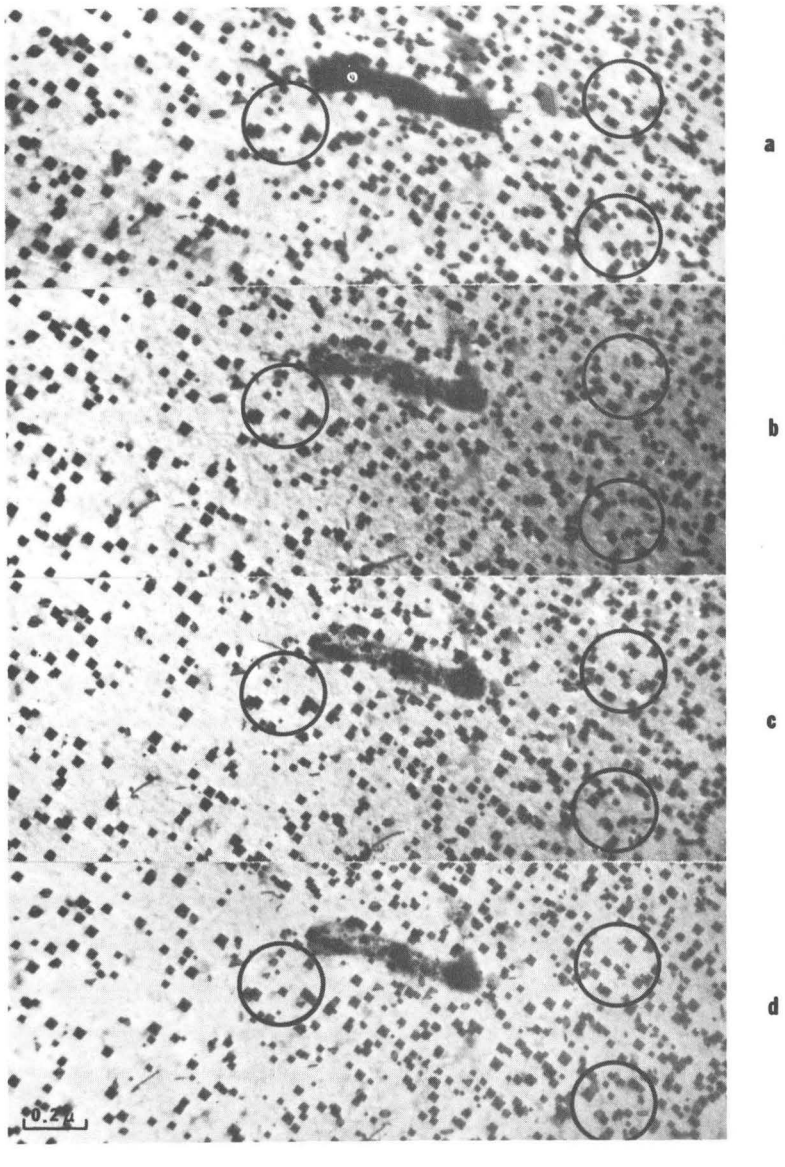

ZN-6033

Fig. 3. Micrographs taken of an area annealed for a) 0, b) 30, c) 60 and d) 90 minutes at 400°C showing the collapse of stacking fault tetrahedra to triangular Frank sessile loops. 0.2μ = 1 cm.

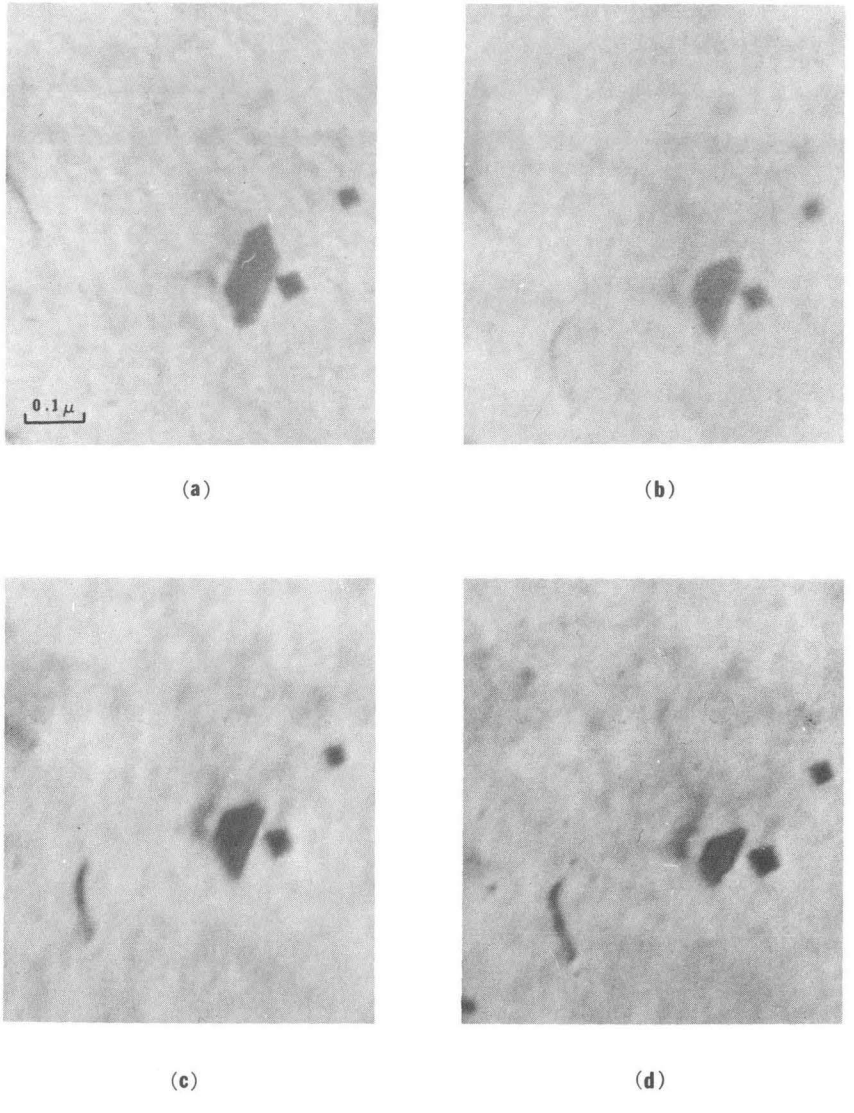

ZN-6037

Fig. 4. Micrographs taken of an area annealed for a) 0, b) 105, c) 165 and d) 225 minutes at 250°C showing the shrinkage of Frank sessile loop. 0.1μ = 1 cm.

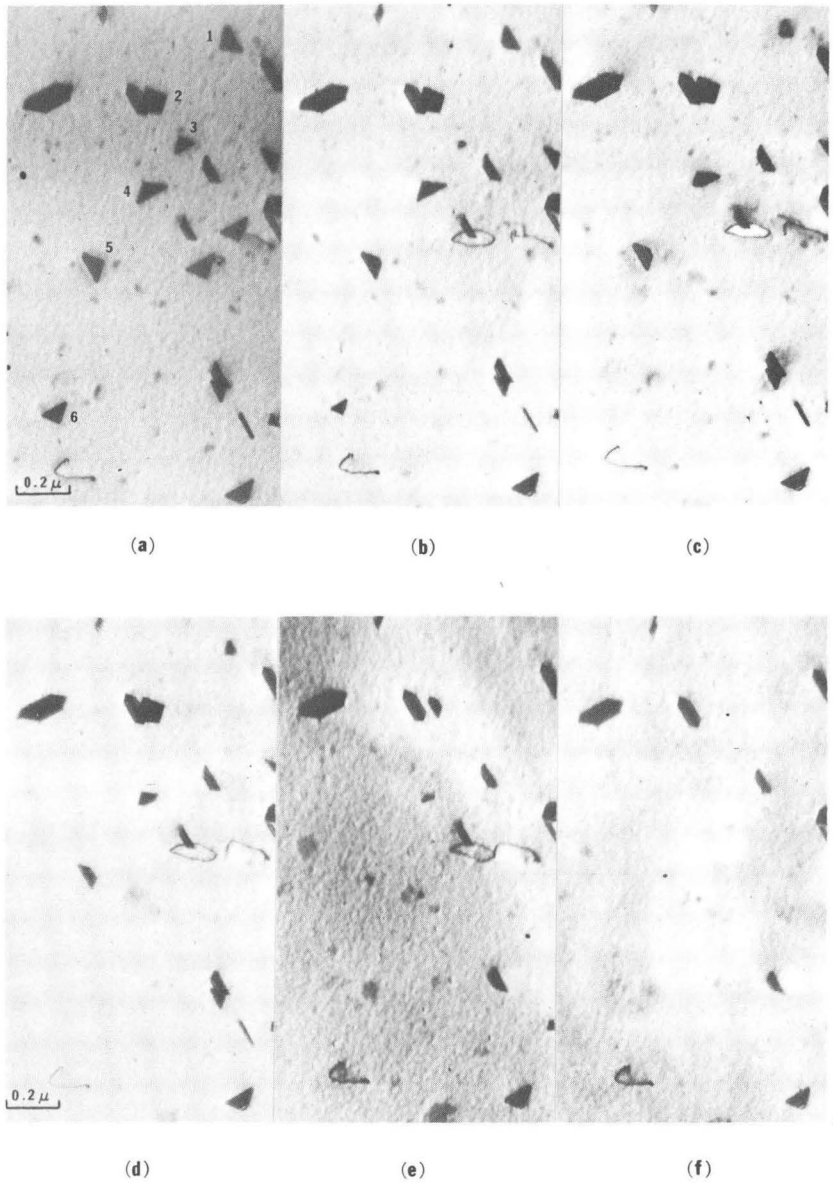

ZN-6034

Fig. 5. Micrographs taken of an area annealed for a) 0, b) 2, c) 4, d) 6, e) 12, and f) 20 hrs. at 300°C showing the complete sequence of the collapse of stacking fault tetrahedra to triangular Frank sessile loops and the subsequent shrinkage of the loops. 0.2 μ = 1 cm.

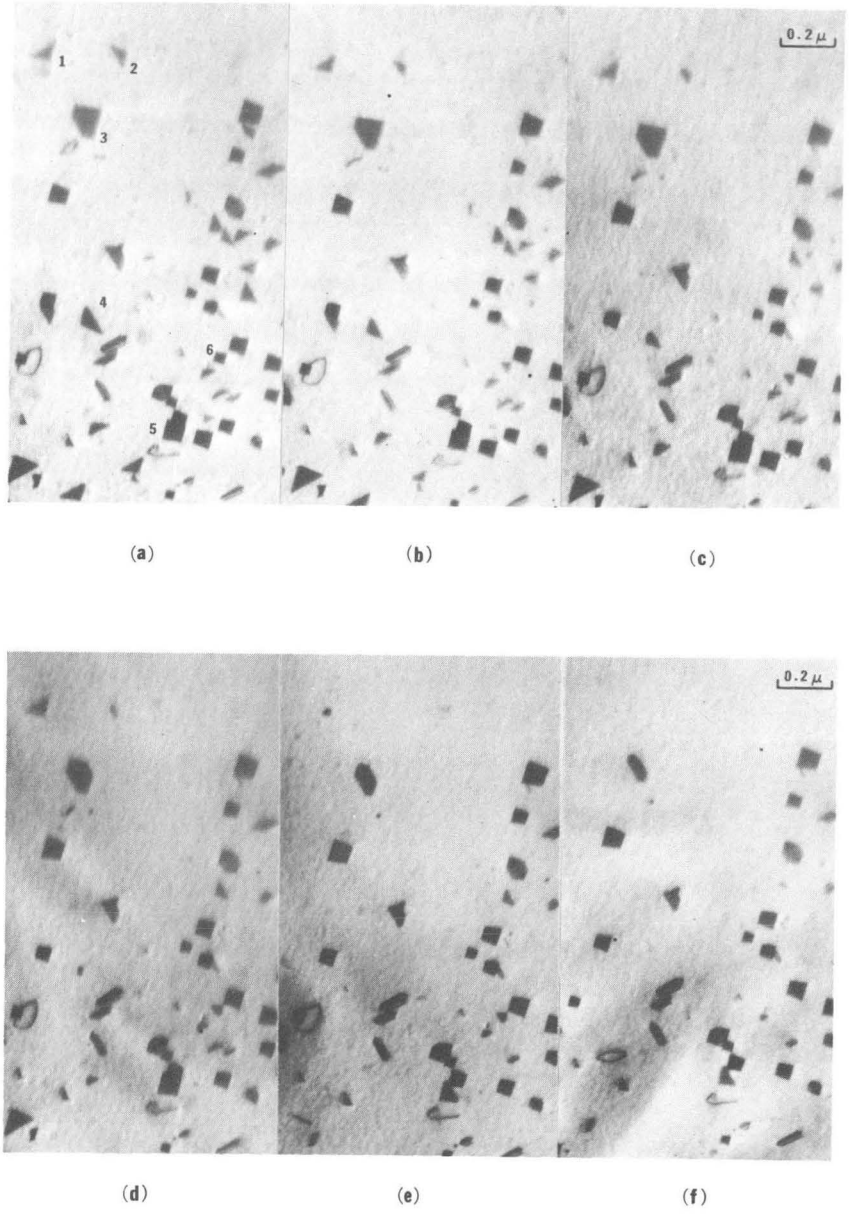

ZN-6035

Fig. 6. Micrographs taken of an area annealed for a) 0, b) 4, c) 10, d) 18, e) 24, and f) 27 hours at 300°C showing the collapse of stacking fault tetrahedra to Frank sessile loops and the subsequent shrinkage of the loops. 0.2μ = 1 cm.

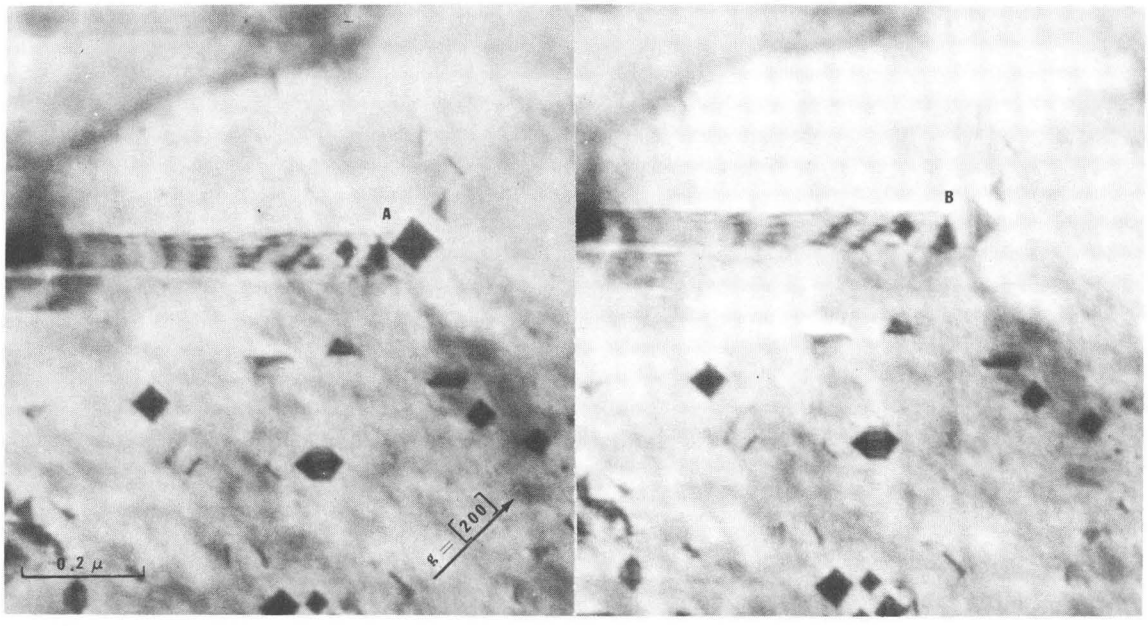

(a) (b)

ZN-6032

Fig. 7. Micrographs of an area taken moments apart showing a non contact interaction of a dislocation with a stacking fault tetrahedron resulting in its collapse to a triangular Frank sessile loop. 0.2μ = 2 cm.

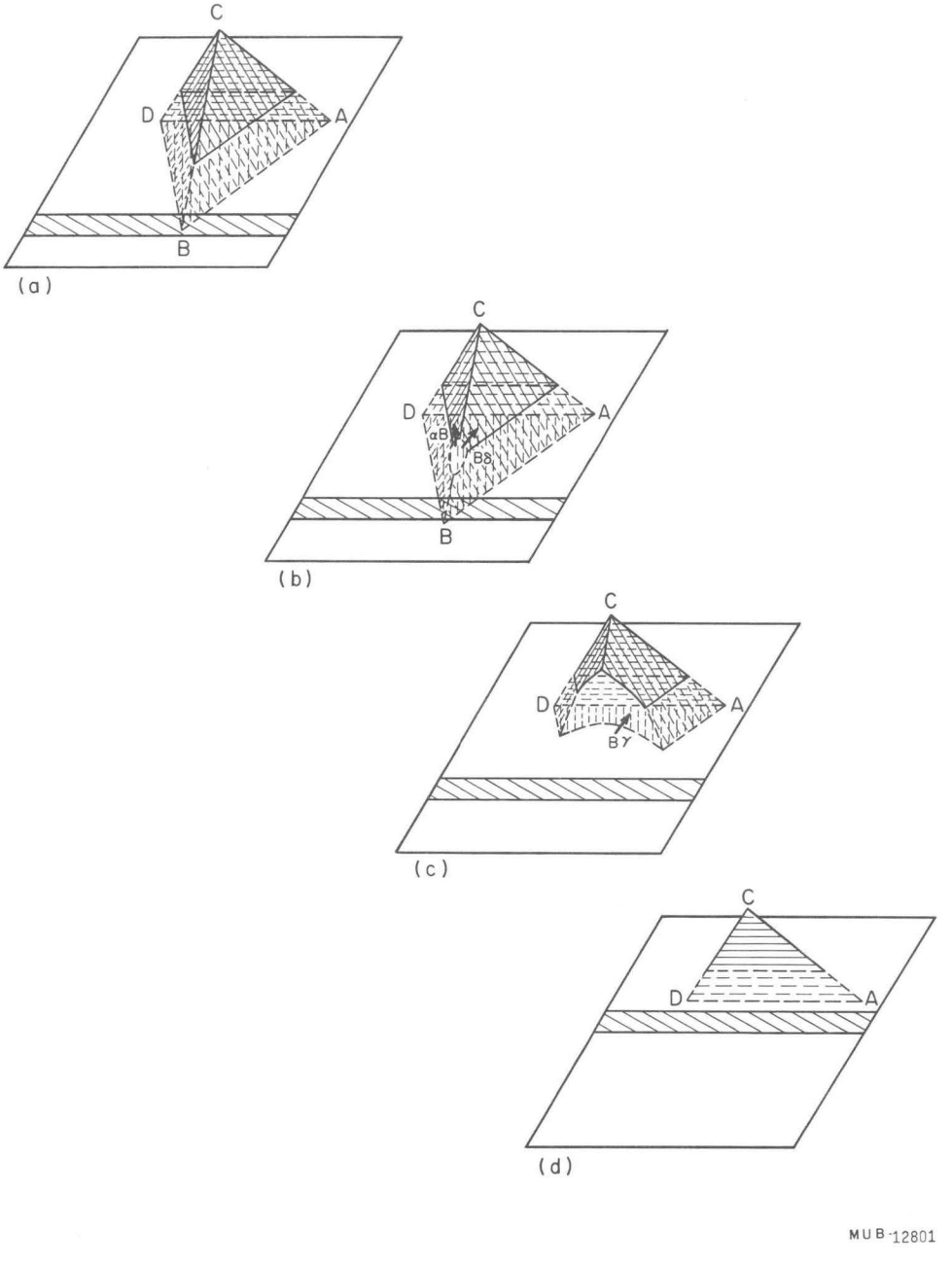

Fig. 8. A sequence of dislocation reactions which can be used to explain the collapse of the stacking fault tetrahedron on Fig. 7.

This report was prepared as an account of Government sponsored work. Neither the United States, nor the Commission, nor any person acting on behalf of the Commission:

A. Makes any warranty or representation, expressed or implied, with respect to the accuracy, completeness, or usefulness of the information contained in this report, or that the use of any information, apparatus, method, or process disclosed in this report may not infringe privately owned rights; or

B. Assumes any liabilities with respect to the use of, or for damages resulting from the use of any information, apparatus, method, or process disclosed in this report.

As used in the above, "person acting on behalf of the Commission" includes any employee or contractor of the Commission, or employee of such contractor, to the extent that such employee or contractor of the Commission, or employee of such contractor prepares, disseminates, or provides access to, any information pursuant to his employment or contract with the Commission, or his employment with such contractor.